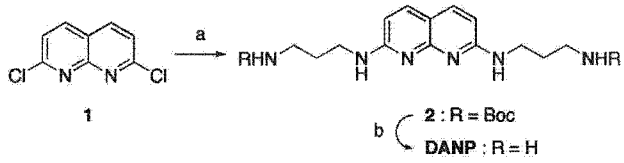

Scheme 1. Reagents and conditions: (a) 1,3-diaminopropane, 60 °C, 24 h, then $(Boc)_2O$, $CHCl_3$, 53%; (b) HCl, EtOAc, $CHCl_3$, quantitative.

product was treated with di-*tert*-butyl dicarbonate to produce Boc-protected DANP. After purification by silica gel column chromatography, the Boc protecting group was removed to give DANP.

The binding of DANP to DNA containing a single nucleotide bulge was examined by measuring melting temperature (T_m) of duplexes 5′-d(TCCAX_YCAAC)-3′/3′-d(AGGTZNWGTTG)-5′ containing a single nucleotide bulge **N**, where **N** was adenine, guanine, cytosine, or thymine. The **X–Z** and **Y–W** were any combinations of Watson–Crick base pairs. Duplexes containing the cytosine bulge in all 16 flanking sequences [4(**X–Z**) × 4(**Y–W**)] were significantly stabilized as judged by the increase of T_m (ΔT_m) in the presence of DANP (100 μM) (ΔT_m = 7.0–12.4 °C) (Fig. 1). The largest ΔT_m (12.4 ° C) was recorded for the duplex 5′-d(TCCA-T_ACAAC)-3′/3′-d(AGGTACTGTTG)-5′ (**T_A/ACT**) where the cytosine bulge was flanked by T–A and A–T base pairs. It was also shown that thymine bulges were effectively stabilized by DANP binding (ΔT_m = 4.7–9.4 °C). In contrast, the T_m increases of guanine (ΔT_m = 3.2–5.6 °C) and adenine (ΔT_m = 2.3–5.7 °C) bulges were less significant as compared to that observed for the cytosine and thymine bulges. It is noteworthy that fully matched duplexes 5′-d(TCCAXYCAAC)-3′/3′-d(AGGTZWGTTG)-5′, where **X–Z** and **Y–W** were any combinations of Watson–Crick base pairs were only weakly stabilized (ΔT_m = 0.5–2.0 °C) under the set conditions (data not shown). These results indicated that DANP showed a preference for the binding to the single pyrimidine bulge over the purine bulge and fully matched duplexes.

The stoichiometry for the binding of DANP to the cytosine and thymine bulge was examined by cold spray ionization time-of-flight mass spectrometry (CSI-TOF MS).[10] In the presence of two molar equivalents of DANP to the cytosine bulge duplex **T_A/ACT**, a distinct ion at *m/z* of 1323.81 and 1654.96 corresponding to 5^- and 4^- ion, respectively, of a 1:1 complex was detected in addition to the intact duplex (Fig. 2). Further increase of the DANP concentration to 6 equiv resulted in an increase of the ion intensity of the 1:1 complex with a concomitant decrease of the intact duplex. Under the conditions, complexes with other binding stoichiometries could not be detected. Similarly, CSI-TOF MS showed a 1:1 complex between DANP and the thymine bulge duplex 5′-d(TCCAT_ACAAC)-3′/3′-d(AGG-TATTGTTG)-5′ (**T_A/ATT**) (Fig. 3). With increasing the amount of DANP, the ion corresponding to the 1:1 complex (*m/z* 1326.42) increased with a concomitant decrease of the ion corresponding to the intact duplex

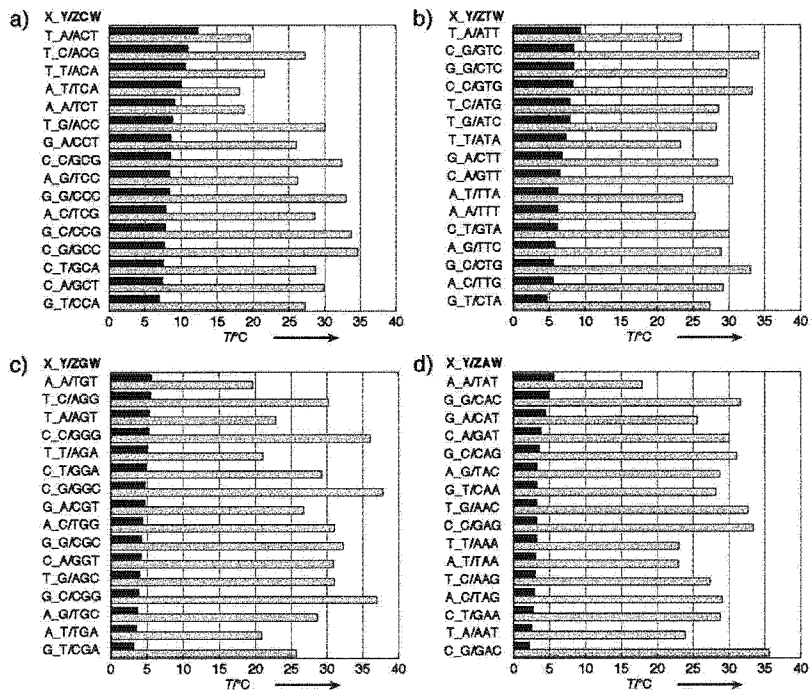

Figure 1. Effects of DANP–binding on the melting temperatures of 5′-d(TCCAX_YCAAC)-3′/3′-d(AGGTZNWGTTG)-5′ containing a single nucleotide bulge (N) flanked by **X–Z** and **Y–W** base pairs. Melting temperature (T_m) of duplex (4.8 μM) measured in sodium cacodylate buffer (pH 7.0, 10 mM) and sodium chloride (100 mM) was shown with a gray bar. Increase of T_m (ΔT_m) in the presence of DANP (100 μM) was shown with a black bar. The flanking base pairs (**X–Z** and **Y–W**) were shown in the left of the bar. Key: (a) C bulge (N = C), (b) T bulge (N = T), (c) G bulge (N = G), and (d) A bulge (N = A).

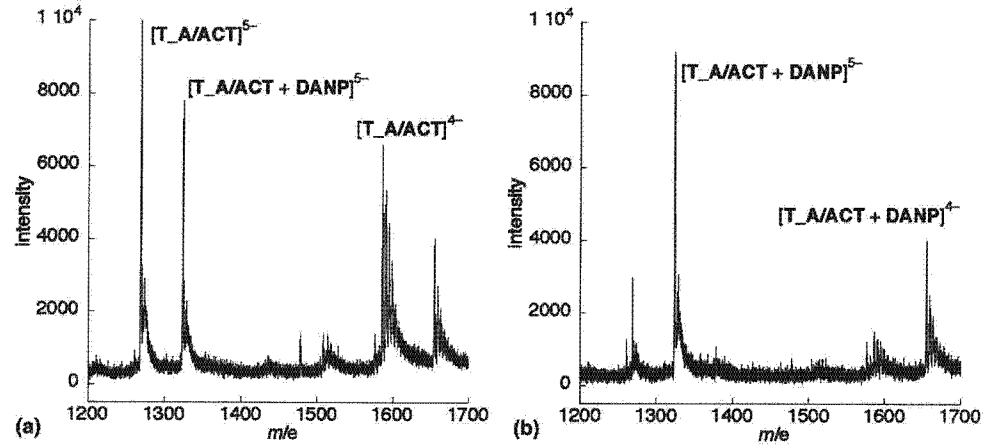

Figure 2. CSI-TOF MS of 5′-d(TCCAT_ACAAC)-3′/3′-d(AGGTACTGTTG)-5′ (T_A/ACT) (20 μM) measured in 50% aqueous methanol and 100 mM ammonium acetate in the presence of (a) 40 and (b) 120 μM of DANP.

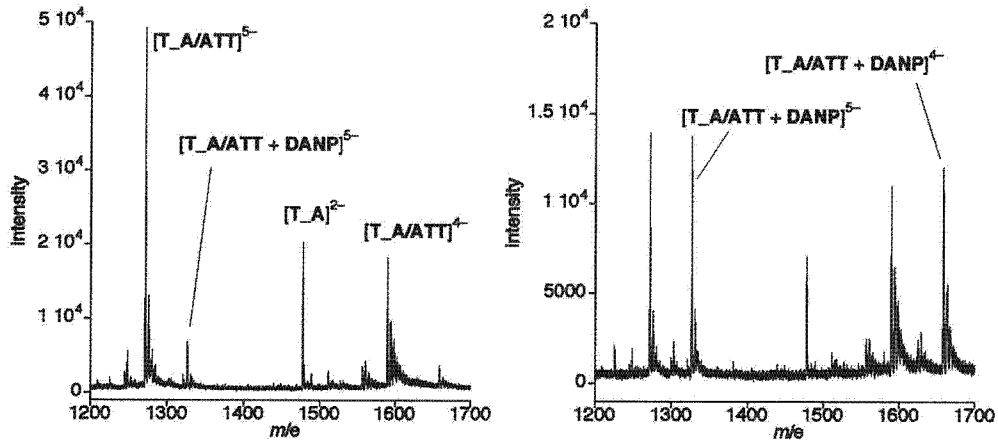

Figure 3. CSI-TOF MS of 5′-d(TCCAT_ACAAC)-3′/3′-d(AGGTATTGTTG)-5′ (T_A/ATT) (20 μM) measured in 50% aqueous methanol and 100 mM ammonium acetate in the presence of (a) 40 and (b) 120 μM of DANP.

(*m/z* 1271.57). These CSI-TOF MS experiments strongly suggested that DANP bound to both cytosine and thymine bulge with a 1:1 stoichiometry. In the presence of 6 equiv of DANP, the ion intensity corresponding to the intact duplex was much higher for the thymine bulge than for the cytosine bulge, suggesting that DANP binding to the cytosine bulge would be stronger than to the thymine bulge. This is consistent with a larger ΔT_m observed for the cytosine bulge than for the thymine bulge in the same T_A/ANT (N = C or T) sequence context. The association constant for the DANP binding to the cytosine bulge was determined to be $7.5 \times 10^5\ M^{-1}$ by fluorescence titration and Scatchard plot analysis (data not shown).

To gain further insight into the DANP binding to the cytosine and thymine bulges, the pH dependency of DANP absorption spectra were examined. Absorption spectra of DANP free in solution were sensitive to the pH of the solution (Fig. 4a). At pH 8.5, the absorption maximum was observed at 365 nm, whereas it shifted to 376 nm at pH 5.0. A plot of the absorbance at 376 nm against the solution pH showed a sigmoid curve (Fig. 4b). The pH dependency of the UV absorbance of DANP was rationalized by a protonation at the nitrogen in a 2,7-diamino-1,8-naphthyridine chromophore. Energy calculation in an aqueous solvent using the Cramer–Truhlar solvation methods with density functional theory (B3LYP/6-31G(d)) indicated that a protonation at *N*1 of the 2,7-diamino-1,8-naphthyridine chromophore was energetically much more favorable by 6.9 kcal/mol than a protonation at the 2-amino group. A pK_a of 6.8 for the protonated form of DANP ($DANPH^+$) was obtained as the pH at the inflection of the curve. A protonation of *N*1 of DANP resulted in the modulation of the hydrogen-bonding surface from an alignment of D–A–A–D in DANP to a D–A–D–D alignment in $DANPH^+$. The D–A–D–D alignment of the hydrogen-bonding groups in $DANPH^+$ is fully complementary not only to that of cytosine (D–A–A) but also to that of thymine base (A–D–A). The complementarily hydrogen bonding surface to that of the cytosine and thymine is most likely to rationalize the selective binding of DANP to pyrimidine bases. In a proposed hydrogen-bonding scheme between $DANPH^+$ and cytosine, the proton attached *N*1 would be bound by *N*3 of

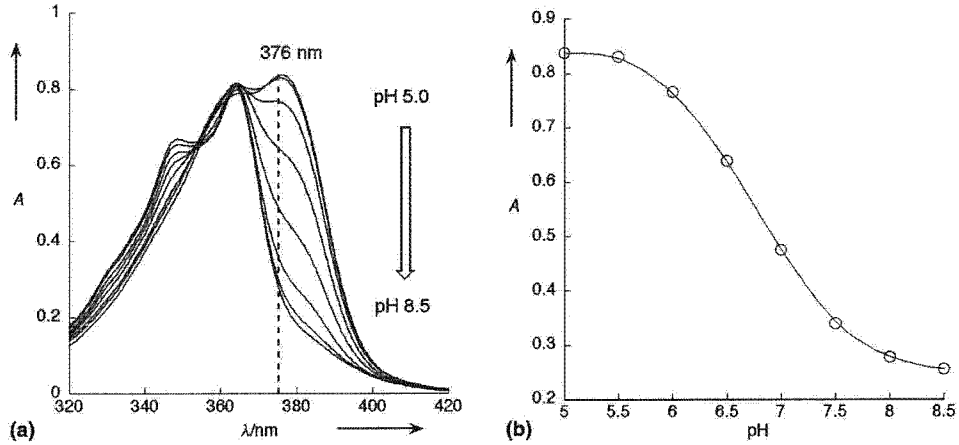

Figure 4. (a) Absorption spectra of DANP (100 μM) recorded at pH of 5.0, 5.5, 6.0, 6.5, 7.0, 7.5, 8.0, and 8.5 in sodium phosphate buffer (10 mM) and sodium chloride (100 mM). (b) A plot of absorption at 376 nm against the solution pH.

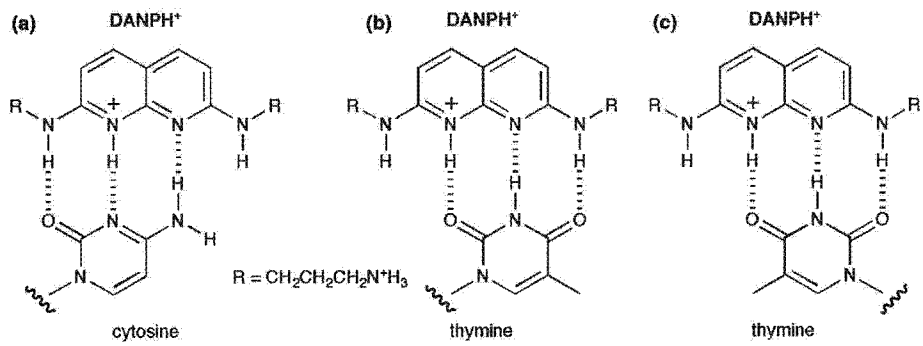

Figure 5. Proposed hydrogen-bonding schemes between $DANPH^+$ and pyrimidine nucleobases. Key: (a) cytosine, (b) and (c) thymine. Two orientations are conceivable for hydrogen bonding of $DANPH^+$ to thymine.

the cytosine. Due to a palindromic A–D–A alignment of hydrogen-bonding groups in the thymine base, two orientations were conceivable for the hydrogen bonding to $DANPH^+$. The difference in the two orientations was that the non-hydrogen bonding amino group was located either in a minor groove (Fig. 5b) or in a major groove of the $DANPH^+$–DNA complex (Fig. 5c).

When aromatic molecules intercalated into DNA, the electronic state of the molecule would be significantly affected by the stacking interaction with the neighboring base pairs. It was confirmed that DANP showed a large spectroscopic change upon binding to a single pyrimidine bulge. The UV absorption was measured with a constant DANP (10 μM) and DNA (30 μM) concentration in phosphate buffer (pH 7.0) and 100 mM NaCl. Free DANP in phosphate buffer (pH 7.0) showed absorption maximum at 364 nm with a shoulder at 376 nm. The presence of fully matched duplex as well as adenine bulge duplex resulted in a small hypochromic shift but not a bathochromic shift of the absorption maximum (Fig. 6a). In contrast, the cytosine bulge duplex (**T_A/ACT**) induced a bathochromic shift by 30 nm to 394 nm with a concomitant hypochromic shift by 65%. Bathochromic shift of DANP absorption was also induced by the thymine bulge (**T_A/ATT**) producing the absorption maximum at 390 nm. Guanine bulge duplex was intermediate between the pyrimidine and adenine bulge duplex in terms of the bathochromic shift. In response to the bathochromic shift, fluorescence spectra of DANP showed a significant change with respect to the emission wavelength and the shape of the spectra. The fluorescence spectra of DANP free in solution excited at its absorption maximum showed an emission maximum at 394 nm in pH 7.0. The emission maximum of DANP was not virtually affected by the presence of fully matched duplex and adenine bulge duplex. However, a broad emission with the emission maximum at 424 nm was observed in the presence of the cytosine bulge. In the presence of thymine bulge, a similar fluorescence spectrum was obtained with a decreased intensity. Quantum yield of DANP fluorescence at 424 nm obtained by an excitation at 394 nm in the presence of **T_A/ACT** and **T_A/ATT** were 0.332 and 0.166, respectively.

The results described here showed that DANP bound not only to the cytosine but also to the thymine bulge. The selective DANP binding to these pyrimidine bulges was most plausible by the protonation of the nitrogen in the 2,7-diamino-1,8-naphthyridine chromophore, producing hydrogen-bonding surfaces fully complementary to those of cytosine and thymine. We have demonstrated that molecules having hydrogen-bonding surface

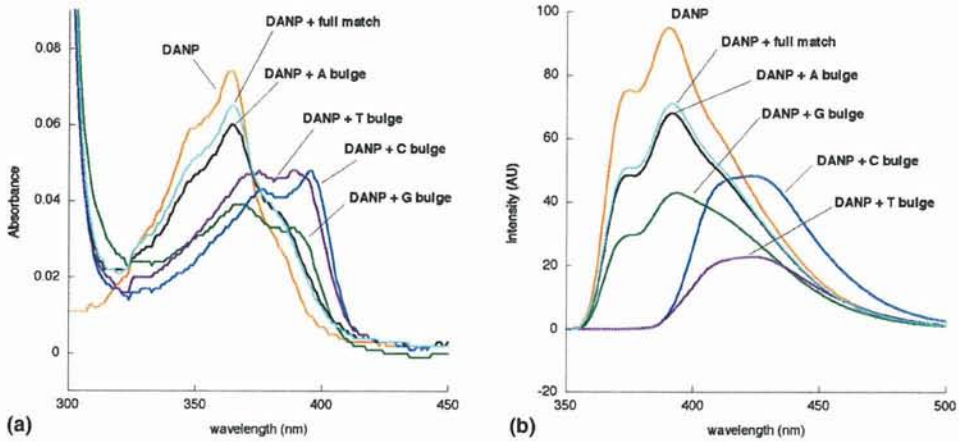

Figure 6. (a) Absorption spectra of DANP (10 μM) recorded in the presence of duplexes 5′-d(TCCAT_ACAAC)-3′/3′-d(AGGTANTGTTG)-5′ containing N bulge (N = C, T, G, and A) (30 μM) and 10-mer fully matched duplexes 5′-d(TCCATACAAC)-3′/3′-d(AGGTATGTTG)-5′ (30 μM) in sodium phosphate buffer (pH 7.0, 10 mM) and sodium chloride (100 mM). (b) Fluorescence spectra of DANP recorded under the same conditions. Excitation wavelength was at the absorption maxima.

fully complementary to the nucleotide bases were useful probes for the detection of bulges and mismatches in duplex DNA. Because, protonation of the nitrogen in heterocycles could effectively modulate the hydrogen-bonding surface from the acceptor to the donor, the idea of the protonation of the chromophore may provide a new way for the design of a molecular element for the base recognition. Furthermore, the observed spectroscopic changes upon binding of DANP to pyrimidine bulges could be applicable to the detection of the single pyrimidine bulge in duplex DNA.

1. Experimental

1.1. {3-[7-(3-{*tert*}-Butoxycarbonylamino-propylamino)-[1,8]naphthyridin-2-ylamino]-propyl}-carbamic acid *tert*-butyl ester (*2*)

A mixture of **1** (50 mg, 0.25 mmol) and 1,3-diaminopropane (2 ml, 23.9 mmol) was stirred at 60 °C for 24 h. The solvent was evaporated in vacuo. The residue was dissolved in chloroform (5 ml) and was added $(Boc)_2O$ (300 mg, 1.37 mmol). The mixture was stirred at 40 °C for 6 h. Solvents were evaporated in vacuo and the resulting solid was purified by silica gel column chromatography ($CHCl_3/CH_3OH$ and hexane/AcOEt) to give **2** (62.9 mg, 53%) as yellow solids: ^1H NMR ($CDCl_3$, 400 MHz) $\delta = 7.54$ (d, 2H, $J = 8.8$ Hz), 6.34 (d, 2H, $J = 8.8$ Hz), 3.58 (q, 4H, $J = 6.0$ Hz), 3.22 (q, 4H, $J = 6.0$ Hz), 1.78 (tt, 4H, $J = 6.0$ Hz), 1.44 (s, 18H); ^{13}C NMR ($CDCl_3$, 100 MHz) $\delta = 159.8$, 157.2, 156.6, 137.3, 110.8, 106.7, 79.3, 38.5, 37.9, 30.7, 28.5 MS (ESI), *m/e* 497 $[M+Na^+]$, 475 $[M+H^+]$; HRMS calcd for $C_{24}H_{39}NaN_6O_4$ $[M+Na^+]$ 497.2852, found 497.2834, $C_{24}H_{39}N_6O_4$ $[M+H^+]$ 475.3033, found 475.2996.

1.2. *N,N′*-Bis-(3-amino-propyl)-[1,8]naphthyridine-2,7-diamine (DANP)

To a $CHCl_3$ (1 ml) solution of (14.5 mg, 30.6 μmol) was added ethyl acetate containing 4 N HCl (2 ml). The mixture was stirred at room temperature for 30 min. Solvent was evaporated to dryness to give DANP (quantitative) as yellow solids: ^1H NMR (CD_3 OD, 400 MHz) $\delta = 7.79$ (d, 2H, $J = 8.8$ Hz), 6.61 (d, 2H, $J = 8.8$), 3.63 (t, 4H, $J = 6.8$ Hz), 3.42 (t, 4H, $J = 7.2$ Hz), 2.04 (tt, 4H, 7.2 Hz); ^{13}C NMR (D_2O, 100 MHz) $\delta = 157.3$, 148.5, 140.6, 109.0, 108.1, 38.6, 37.4, 26.6. MS (FAB), *m/e* 275 $[(M+H)^+]$; HRMS calcd for $C_{14}H_{23}N_6$ $[(M+'H)^+]$ 275.1984, found 275.1987.

1.3. Measurements of melting temperature of bulge-containing duplexes

DANP (100 μM) was dissolved in a sodium cacodylate (10 mM, pH 7.0) containing bulge duplex (4.8 μM) and NaCl (100 mM). The mixture was heated at 50 °C and cooled slowly to make sure that the starting oligomers is in a duplex state. The thermal denaturation profile was recorded on a SHIMADU UV2550 spectrometer equipped with a SHIMADU TMSPC-8 temperature controller. The absorbance of the sample was monitored at 260 nm from 4 to 70 °C with a heating rate of 1 °C/min.

1.4. CSI-TOF measurements

Samples were prepared by mixing DNA (20 μM) and DANP (40 and 120 μM) in 50% methanol in water containing 100 mM NH_4OAc. Mass spectra were obtained with a JEOL JMS-T100 mass spectrometer equipped with cold spray ion source. Spray temperature was set at −10 °C with a sample flow rate of 10 μL/min.

1.5. UV and fluorescent spectra measurements

UV spectra were recorded on a SHIMADU UV2550 spectrometer. Fluorescent spectra were recorded on a SHIMADU RF-5300PC. DNA samples were prepared in 10 mM sodium phosphate buffer at the designate pH in the presence of 100 mM sodium chloride. Excitation wavelength for the fluorescent measurements was the wavelength at the absorption maximum unless otherwise noted.

References and notes

1. Guest, C. R.; Hochstrasser, R. A.; Sowers, L. C.; Millar, D. P. *Biochemistry* **1991**, *30*, 3271.
2. Stivers, J. T. *Nucleic Acids Res.* **1998**, *26*, 3837.
3. Hawkins, M. E.; Balis, F. M. *Nucleic Acids Res.* **2004**, *32*, e62.
4. Nakatani, K. *ChemBioChem.* **2004**, *5*, 1623.
5. Nakatani, K.; Sando, S.; Saito, I. *Nat. Biotechnol.* **2001**, *19*, 51.
6. Hagihara, S.; Kumasawa, H.; Goto, Y.; Hayashi, G.; Kobori, A.; Saito, I.; Nakatani, K. *Nucleic Acids Res.* **2004**, *32*, 278.
7. Yoshimoto, K.; Nishizawa, S.; Minagawa, M.; Teramae, N. *J. Am. Chem. Soc.* **2003**, *125*, 8982.
8. Kobori, A.; Horie, S.; Suda, H.; Saito, I.; Nakatani, K. *J. Am. Chem. Soc.* **2004**, *126*, 557.
9. George, R. N.; Sam, J. G.; Veronica, K. M.; Frank, R. F.; Giacomo, C. *J. Org. Chem.* **1981**, *46*, 833.
10. Yamaguchi, K. *J. Mass. Spectrom.* **2003**, *38*, 473.

DNA Cleavage

DOI: 10.1002/anie.200502282

Binding of Naphthyridine Carbamate Dimer to the $(CGG)_n$ Repeat Results in the Disruption of the G–C Base Pairing

*Tao Peng and Kazuhiko Nakatani**

The expansion of the $(CGG)_n$ trinucleotide repeat in the FMR1 gene causes the neurological disorder fragile X syndrome.[1–3] The molecular basis for the $(CGG)_n$ expansion involves the formation of a metastable hairpin structure[4–6] consisting of continued 5′-CGG-3′/5′-CGG-3′ triads, in which a G–G mismatch is flanked by two G–C base pairs. We recently reported the remarkable binding of naphthyridine azaquinolone (**NA**) to the 5′-CAG-3′/5′-CAG-3′ triad in the hairpin form of the $(CAG)_n$ repeat, where the A–A mismatch was flanked by G–C base pairs. The ligand-bound structure was intriguing because 1) two **NA** molecules were bound to a single CAG/CAG triad which 2) induced the cytosine—which was hydrogen-bonded to the guanine—to flip out from the base stack (Figure 1).[7] The **NA**-immobilized sensor was useful for the rapid diagnosis of the $(CAG)_n$ repeat length. We have reported a series of ligands binding to a G–G mismatch,[8–10] and therefore the remarkable structure of **NA** bound to the CAG/CAG triad prompted us to investigate the mode of ligand binding to the CGG/CGG triad and, hence, the possibility of the cytosine flipping out in the ligand-bound complex. Herein, we report that naphthyridine carbamate dimer (**NC**)[11] binds to a single CGG/CGG triad with exclusively 2:1 **NC**/triad stoichiometry. The binding of **NC** to the CGG/CGG triad induced the disruption of the guanine–cytosine base pairing in the triad, and made the cytosine susceptible to the subsequent chemical cleavage reaction initiated by addition of hydroxylamine.

Among the ligands that we synthesized for binding to the G–G mismatch, **NC** showed a marked preference in binding to the CGG/CGG triad. The binding of **NC** to the CGG/CGG triad in the 13-mer duplex increased the melting temperature (T_m) by 23.1 °C, whereas the increase in T_m (ΔT_m) was only 6.7 °C for the GGC/GGC triad (Table 1). A survey of the effect of the flanking sequence suggested that the strong and selective **NC** binding to the CGG/CGG triad is most likely a consequence of the interaction of **NC** not only with the G–G mismatch, but also with the cytosine on the 5′ side and/or the guanine on the 3′ side.

[*] T. Peng, Prof. K. Nakatani
The Institute of Scientific and Industrial Research
Osaka University
Ibaraki 567-0047 (Japan)
Fax: (+81) 6-6879-8459
E-mail: nakatani@sanken.osaka-u.ac.jp

Supporting information for this article is available on the WWW under http://www.angewandte.org or from the author.

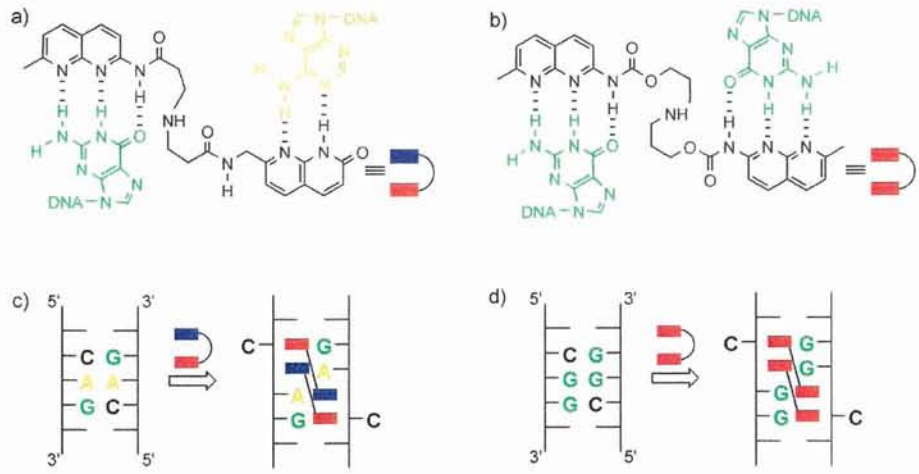

Figure 1. Hydrogen-bonding between a) **NA** and the G–A mismatch and b) **NC** and the G–G mismatch. Schematic illustrations of c) the NMR-confirmed **NA**-CAG/CAG triad complex and d) the proposed **NC** binding to the CGG/CGG triad. Red rectangles: 2-amino-1,8-naphthyridine; blue rectangles: 8-azaquinolone.

Table 1: ΔT_m [°C] and ΔT_m values [°C] for the 13-mer duplexes containing a G–G mismatch in a different flanking sequence.[a]

5′-GCTAA XGZ AATGA-3′
3′-CGATT YGW TTACT-5′

5′-XGZ-3′/5′-WGY-3′	$T_m(-)$[b]	$T_m(+)$[c]	ΔT_m[d]
CGG/CGG	34.1 (0.9)	57.2 (0.4)	23.1 (0.4)
CGC/GGG	38.6 (0.1)	49.3 (0.8)	10.7 (0.8)
GGC/GGC	40.4 (0.3)	47.1 (1.4)	6.7 (1.4)
CGA/TGG	31.8 (0.2)	44.4 (0.3)	12.6 (0.3)
CGT/AGG	33.6 (0.2)	44.0 (0.5)	10.4 (0.5)
GGA/TGC	34.2 (0.3)	43.4 (0.4)	9.2 (0.4)
AGT/AGT	28.7 (0.4)	41.9 (1.0)	13.2 (1.0)
AGG/CGT	31.8 (0.6)	39.9 (0.8)	8.1 (0.8)
GGT/AGC	33.7 (0.4)	39.3 (0.3)	5.6 (0.3)
TGA/TGA	17.8 (0.4)	35.9 (1.0)	18.1 (1.0)

[a] The UV melting curve was measured for a duplex (4.5 μM) in a sodium cacodylate buffer (10 mM, pH 7.0) containing NaCl (100 mM). The temperature was increased at a rate of 1 K min^{-1}. All measurements were made three times, and standard deviations are shown in parentheses. [b] T_m values of oligomers. [c] T_m values of oligomers in the presence of **NC** (100 μM). [d] ΔT_m was calculated as the difference between $T_m(+)$ and $T_m(-)$.

To determine the stoichiometry of the **NC**-CGG/CGG complex, cold-spray ionization time-of-flight mass spectrometry (CSI-TOF MS)[12] of the 11-mer self-complementary duplex containing the CGG/CGG triad was carried out (Figure 2). In the absence of **NC**, three ions derived from the oligomer were observed. One ion corresponded to the 3– ion of a single-stranded form ($[ss]^{3-}$; *m/z*: found 1118.13, calcd 1117.19). Duplexes were detected as a 5– ion ($[G–G]^{5-}$; *m/z*: found 1342.32, calcd 1340.83) and a 4– ion ($[G–G]^{4-}$; *m/z*: found 1678.07, calcd 1676.29). Upon addition of **NC** to the duplex with a 1:1 molar ratio, the intensity of the ions corresponding to $[ss]^{3-}$, $[G–G]^{5-}$, and $[G–G]^{4-}$ became weak, with the concomitant appearance of a new ion corresponding to the 5– ion of a 2:1 complex of **NC** and the duplex ($[G–G+2NC]^{5-}$; *m/z*: found 1544.13, calcd 1542.13). A 1:1 complex was not detected. In the presence of two equivalents of **NC**, ions derived from the free duplex disappeared and only $[G–G+2NC]^{5-}$ was detected. At an increased concentration of **NC**, the ion corresponding to $[G–G+2NC]^{5-}$ was still predominant. These results clearly show that the binding of **NC** to the duplex containing the CGG/CGG triad proceeded exclusively with a 2:1 stoichiometry. The binding of **NC** to the CGG/CGG triad was further characterized by UV absorption titration experiments (see the Supporting Information). The crossover point of the Job's plot obtained from the titration was at 66%, which confirmed that the binding stoichiometry of **NC** to the CGG/CGG triad was 2:1, as determined by CSI-TOF MS (see the Supporting Information).

The high sequence preference and the 2:1 stoichiometry for **NC** binding are the same characteristic features that we observed for the binding of **NA** to the CAG/CAG triad.[7] Encouraged by these facts, we investigated whether the

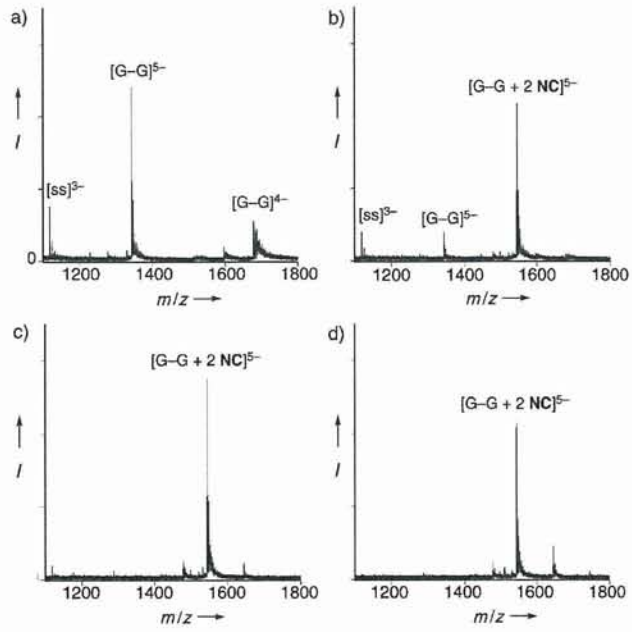

Figure 2. CSI-TOF MS of 11-mer self-complementary duplex 5′-d(TCAA CGG TTGA)-3′/5′-d(TCAA CGG TTGA)-3′ containing the CGG/CGG triad. Samples contained 20 μM duplex in 50% aqueous methanol and 100 mM ammonium acetate. The sample solution was cooled at −10°C during injection at a flow rate of 0.5 mL h^{-1}. a) Duplex only; b)–d) duplex with 20, 40, and 60 μM **NC**, respectively.

cytosine in the CGG/CGG triad was free from the G–C base pairing upon **NC** binding. We examined the reaction of **NC**-bound CGG/CGG triad with hydroxylamine. Cytosines in the single-stranded regions and in the mismatched base pairs efficiently reacted with two molecules of hydroxylamine at the C4 and C6 positions, whereas those in the G–C base pair in a duplex were not susceptible to the addition of hydroxylamine. The cytosine modified with hydroxylamine underwent degradation on heating with piperidine, eventually leading to strand cleavage.[13]

The reaction of 11-mer self-complementary 5′-d(TCAA CGG TTGA)-3′ (**1**) with hydroxylamine was monitored by reversed-phase HPLC (Figure 3). The duplex of **1**

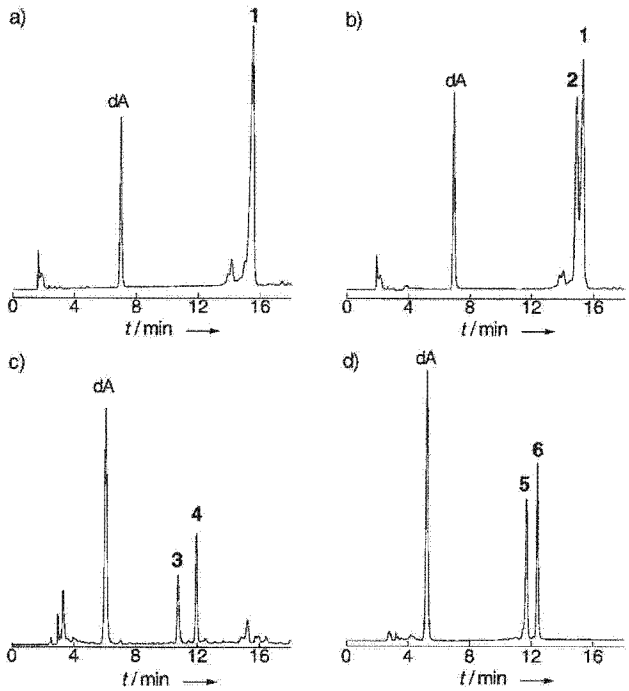

Figure 3. HPLC profiles for the hydroxylamine-induced cleavage at the cytosine moiety in the CGG/CGG triad. The 11-mer self-complementary oligomer 5′-d(TCAA CGG TTGA)-3′ (**1**) (13 μM as a duplex) in NaCl (100 mM) was treated with hydroxylamine (2.8 M, pH 6.0) in the a) absence and b) presence of **NC** (40 μM) at 0 °C for 12 h. c) Product **2** was isolated and treated with piperidine at 90 °C for 30 min. d) Products **3** and **4** were treated with alkaline phosphatase at 37 °C for 2 h. Deoxyadenosine (dA) was added as an internal standard.

(13 μM) was not reactive toward hydroxylamine (2.8 M, pH 6.0) at 0 °C for 12 h, whereas a new product **2** was produced in the presence of **NC** (40 μM). A prolonged reaction time (≈24 h) resulted in 70% consumption of **1** without the formation of any major by-products (see the Supporting Information), which suggests that both strands of **1** duplex reacted with hydroxylamine and produced **2**. MALDI-TOF MS showed that product **2** was the adduct of **1** with two molecules of hydroxylamine (*m/z*: found 3406.06, calcd 3403.62; see Scheme 1 and the Supporting Information).[13] After isolation by HPLC, product **2** was treated with piperidine at 90 °C for 30 min to give products **3** and **4**. The

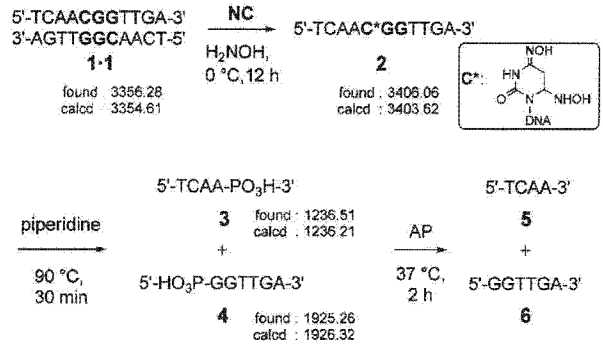

Scheme 1. Hydroxylamine-induced cleavage at cytosine in the **NC**-bound CGG/CGG triad. AP = alkaline phosphatase.

MALDI-TOF mass spectra showed that **3** was the oligomer 5′-d(TCAA)-PO_3H-3′ (*m/z*: found 1236.51, calcd 1236.21), whereas **4** was the oligomer 5′-HO_3P-d(GGTTGA)-3′ (*m/z*: found 1925.26, calcd 1926.32). The phosphorylated termini of **3** and **4** were removed by treatment with alkaline phosphatase to give 5′-d(TCAA)-3′ (**5**) and 5′-d(GGTTGA)-3′ (**6**), respectively. The oligomers **5** and **6** showed the same retention times as authentic oligomers, as observed by co-injection in reversed-phase HPLC. These HPLC analyses clarified that the cytosine in the CGG/CGG triad in **1** duplex became susceptible to the hydroxylamine upon binding with **NC**. The **1** duplex contained two kinds of cytosine, one in the CGG/CGG triad and the other in 5′-TCA-3′/5′-TGA-3′. The cytosine in the latter sequence was insensitive to hydroxylamine, regardless of the presence of **NC**. These results showed that the binding of **NC** to the CGG/CGG triad made the cytosine free from the base pairing to the guanine moiety in the opposite strand.

CSI-TOF MS measurements suggested that the 2:1 **NC**-CGG/CGG complex, which was confirmed for an oligomer duplex, was also produced in the $(CGG)_n$ repeat. CSI-TOF MS of $d(CGG)_{10}$ with **NC** showed the ions corresponding to $[d(CGG)_{10}+6\mathbf{NC}]^{6-}$ and $[d(CGG)_{10}+6\mathbf{NC}]^{7-}$, which suggests the formation of the 2:1 **NC**-CGG/CGG triad complex in the $d(CGG)_{10}$ repeat (see the Supporting Information). In addition, a large conformational change of $d(CGG)_{10}$ was observed in CD measurements upon binding with **NC** (see the Supporting Information), which supports the formation of a hairpin structure, as observed in the binding of **NA** to $d(CAG)_{10}$.[7]

In summary, the data presented herein have shown that 1) **NC** is the first molecule to bind to the CGG/CGG triad, and 2) the cytosine in the triad is free from hydrogen bonding to the guanine moiety upon **NC** binding. It is suggested that the 2:1 **NC**-CGG/CGG complex is produced in the hairpin structure of the $d(CGG)_n$ repeat, which is proposed to form in the replication leading to the repeat expansion. From the structural viewpoint, the **NC**-bound CGG repeats are particularly interesting. Base flipping as a result of the disruption of base pairing is one of the mechanisms for the repair enzyme to recognize the damaged bases and mismatched base pairs.[14–17] Therefore, **NC** could be a useful molecule for studying not only the repeat expansion mechanism, but also

the nucleobase–ligand interactions on the biologically important repeat sequence.

Received: June 30, 2005
Revised: August 20, 2005
Published online: October 17, 2005

Keywords: DNA cleavage · mass spectrometry · nucleotides

[1] S. T. Warren, C. T. Ashley, *Annu. Rev. Neurosci.* **1995**, *18*, 77–99.
[2] R. D. Wells, S. T. Warren, *Genetic Instabilities and Hereditary Neurological Diseases*, Academic Press, New York, **1998**.
[3] A. Brussino, C. Gellera, A. Saluto, C. Mariotti, C. Arduino, B. Castellotti, M. Camerlingo, V. de Angelis, L. Orsi, P. Tosca, N. Migone, F. Taroni, A. Brusco, *Neurology* **2005**, *64*, 145–147.
[4] A. M. Gacy, G. Goellner, N. Juranic, S. Macura, C. T. McMurray, *Cell* **1995**, *81*, 533–540.
[5] K. Ohshima, R. D. Wells, *J. Biol. Chem.* **1997**, *272*, 16798–16806.
[6] A. M. Paiva, R. D. Sheardy, *J. Am. Chem. Soc.* **2005**, *127*, 5581–5585.
[7] K. Nakatani, S. Hagihara, Y. Goto, A. Kobori, M. Hagihara, G. Hayashi, M. Kyo, M. Nomura, M. Mishima, C. Kojima, *Nat. Chem. Biol.* **2005**, *1*, 39–43.
[8] K. Nakatani, S. Sando, I. Saito, *Nat. Biotechnol.* **2001**, *19*, 51–55.
[9] K. Nakatani, S. Sando, H. Kumasawa, J. Kikuchi, I. Saito, *J. Am. Chem. Soc.* **2001**, *123*, 12650–12657.
[10] K. Nakatani, S. Sando, I. Saito, *Bioorg. Med. Chem.* **2001**, *9*, 2381–2385.
[11] T. Peng, T. Murase, Y. Goto, A. Kobori, K. Nakatani, *Bioorg. Med. Chem. Lett.* **2005**, *15*, 259–262.
[12] K. Yamaguchi, *J. Mass Spectrom.* **2003**, *38*, 473–490.
[13] B. H. Johnston, *Methods Enzymol.* **1992**, *212*, 180–194.
[14] R. J. Roberts, X. Chen, *Annu. Rev. Biochem.* **1998**, *67*, 181–198.
[15] E. Seibert, J. B. A. Ross, R. Osman, *J. Mol. Biol.* **2003**, *330*, 687–703.
[16] D. S. Daniels, T. T. Woo, K. X. Luu, D. M. Noll, N. D. Clarke, A. E. Pegg, J. A. Tainer, *Nat. Struct. Mol. Biol.* **2004**, *11*, 714–720.
[17] C. Cao, Y. L. Jiang, J. T. Stivers, F. Song, *Nat. Struct. Mol. Biol.* **2004**, *11*, 1230–1236.

Nucleic Acids Symposium Series No. 49 39–40

Molecular labeling of the CGG trinucleotide repeat

Tao Peng and Kazuhiko Nakatani*

The Institute of Scientific and Industrial Research, Osaka University, Ibaraki 567-0047, Japan

ABSTRACT

The new molecular ligand naphthyridine carbamate dimer (NC), possessing 2-amino-1,8-naphthyridines and a carbamate linker, specially binds to guanine–guanine (G–G) mismatch in duplex DNA. The results of T_m measurements showed that NC selectively bound to CGG/CGG triad with high ΔT_m of 23.1 °C. The exclusive stoichiometry 2:1 of the complex of NC with CGG/CGG triad, obtained by the measurements of cold spray ionization time-of-flight mass spectrometry (CSI-TOF MS), showed that NC bound to CGG/CGG triad strongly with two molecules.

INTRODUCTION

Fragile X syndrome is the most commonly inherited form of mental retardation. The fragile X gene (FMR1) was characterized and found to contain a tandem repeated trinucleotide sequence (CGG) near its 5' end.[1] The molecular basis for the (CGG)n expansion is proposed to involve the formation of a metastable hairpin structure in a leading strand during the replication.[2] The hairpin structure of (CGG)n is consisted of continued 5'-CGG-3'/5'-CGG-3' triads, where a G-G mismatch was flanked by two C-G base pairs. We have synthesized several small molecular ligands which could bind to the particular triad sequence to molecularly label the (CGG)n repeat sequence.[3,4] We here report NC strongly binds to the CGG/CGG triad.

RESULTS AND DISCUSSION

NC was synthesized as shown in Scheme 1. Firstly, *N*-Boc-Di-propanolamine was reacted with *N,N'*-disuccinimidyl carbonate (DSC) in dry acetonitrile to produce carbonate **2**.[5] Then **2** was reacted with 2-amino-7-methyl-1,8-naphthyridine to afford Boc-protected **NC**. At last, deprotection by hydrogen chloride in ethyl acetate gave hydrochloride salt of **NC**.

After synthesized the target compound **NC**, the selective binding of **NC** to the G-G mismatch was studied. The assay was carried out by measuring the melting temperature (T_m) of 13-mer duplex 5'-d(GCTAA **xGz** AATGA)-3'/5'-d(TCATT **wGy** TTAGC)-3' containing a G-G mismatch flanked by any combination of Watson-Crick base pairs (Table 1). The ΔT_m values obtained for these sequences were highly dependent on the base pairs flanking the G-G mismatch. The largest ΔT_m value of 23.1 °C was recorded for 5'-**cGg**-3'/5'-**cGg**-3'

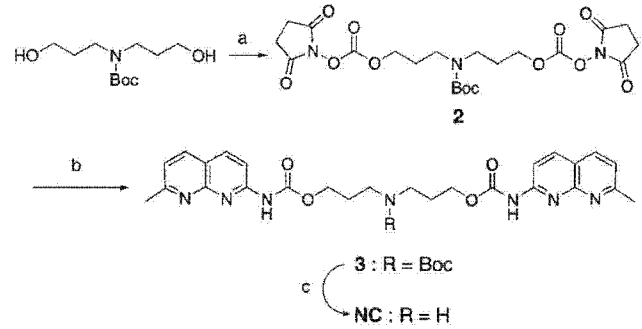

Scheme 1. Reagents and conditions: (a) *N,N'*-disuccinimidyl carbonate, CH_3CN, Et_3N; (b) 2-amino-7-methyl-1,8-naphthyridine, CH_2Cl_2, Et_3N, 49% for 2 steps; (c) HCl, AcOEt, $CHCl_3$, quantitative.

mismatch, whereas only small ΔT_m value was obtained for GGC/GGC (6.1 °C) and GGT/AGC (5.6 °C). **NC**-binding increased the T_m of CGC/GGG and CGA/TGG by 10.7 °C and 12.6 °C, respectively, suggesting that 5' side C and /or 3' side G to the G-G mismatch would be important for **NC**-binding to the G-G mismatch. While large T_m increase was observed for AGT/AGT and TGA/TGA, it is due to the low T_m value of the oligomer alone.

Table 1. Melting Temperature (T_m/°C) of the 13-mer Duplex Containing a G-G mismatch in Different Flanking Sequences in the Absence and Presence of **NC** [a]

5'-GCTAAxGzAATGA-3'
3'-CGATTyGwTTACT-5'

5'-xGz-3'/5'-wGy-3'	T_m(–)[b]	T_m(+)[c]	ΔT_m[d]
cGg/cGg	34.1 (0.9)	57.2 (0.4)	23.1 (0.4)
cGc/gGg	38.6 (0.1)	49.3 (0.8)	10.7 (0.8)
gGc/gGc	40.4 (0.3)	47.1 (1.4)	6.7 (1.4)
cGa/tGg	31.8 (0.2)	44.4 (0.3)	12.6 (0.3)
cGt/aGg	33.6 (0.2)	44.0 (0.5)	10.4 (0.5)
gGa/tGc	34.2 (0.3)	43.4 (0.4)	9.2 (0.4)
aGt/aGt	28.7 (0.4)	41.9 (1.0)	13.2 (1.0)
aGg/cGt	31.8 (0.6)	39.9 (0.8)	8.1 (0.8)
gGt/aGc	33.7 (0.4)	39.3 (0.3)	5.6 (0.3)
tGa/tGa	17.8 (0.4)	35.9 (1.0)	18.1 (1.0)

[a] The UV-melting curve was measured for a duplex (4.5 μM) in a 10 mM sodium cacodylate buffer (pH 7.0) containing 100 mM NaCl. Temperature was increased at a rate of 1 °C/min. All measurements were taken in three times, and standard deviations are shown in the parentheses. [b] T_m values of oligomers. [c] T_m values of oligomers in the presence of **NC** (100 μM). [d] ΔT_m was calculated as a difference of T_m(+) and T_m(–).

Cold spray ionization time-of-flight mass spectrometry (CSI-TOF MS) of 11-mer self-complementary duplex 5'-d(TCAA **CGG** TTGA)-3'/5'-d(TCAA **CGG** TTGA)-3'containing the CGG/CGG triad was measured in theabsence and presence of **NC** to directly observe the **NC**-CGG/CGG complex (Figure 1). Three ions derived from the oligomer were detected without **NC**. One ion was corresponding to a 3– ion of a single stranded form ($[\mathbf{ss}]^{3-}$) (m/z, found 1118.13; calcd. 1117.19). The other two ions were detected as a 5– ion of duplexes ($[\mathbf{G\text{-}G}]^{5-}$) (found 1342.32; calcd. 1340.83) and a 4– ion of duplexes ($[\mathbf{G\text{-}G}]^{4-}$) (found 1678.07; calcd. 1676.29), respectively. In the presence of one molar equivalent of **NC**, only one new ion (found 1544.13; calcd. 1542.13) corresponding to the 5– ion of a 2:1 complex of **NC** and the duplex ($[\mathbf{G\text{-}G} + 2\mathbf{NC}]^{5-}$) appeared. The intensity of the ions of $[\mathbf{ss}]^{3-}$, $[\mathbf{G\text{-}G}]^{5-}$, and $[\mathbf{G\text{-}G}]^{4-}$ became weak at the same time. With two molar equivalents of **NC**, ions derived from free duplex were disappeared and only $[\mathbf{G\text{-}G} + 2\mathbf{NC}]^{5-}$ was detected. Under the increased concentration of **NC**, the ion corresponding to $[\mathbf{G\text{-}G} + 2\mathbf{NC}]^{5-}$ was still predominant. These results clearly showed that the binding of **NC** to the duplex containing the

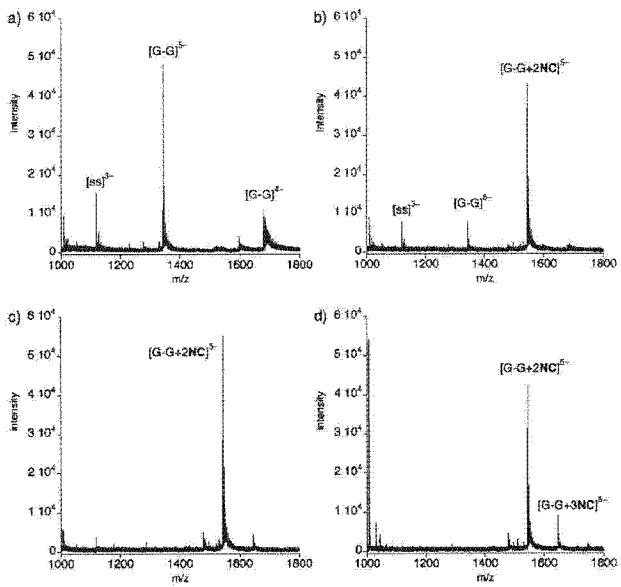

CGG/CGG triad proceeded in an exclusive stoichiometry of 2:1.

Figure 1. CSI-TOF mass spectra of 11-mer self-complementary duplex 5'-d(TCAA **CGG** TTGA)-3'/5'-d(TCAA **CGG** TTGA)-3' containing the CGG/CGG triad in the absence and presence of **NC**. Samples contained 20 μM duplex in 50% aqueous methanol and 100 mM ammonium acetate. For clarity, the range of m/z from 1000 to 1800 was shown. The sample solution was cooled at –10 °C during the injection with a flow rate of 0.5 mL/h. Key: (a) duplex only; (b) duplex with 20 μM **NC**; (c) duplex with 40 μM **NC**; (d) duplex with 60 μM **NC**.

CSI-TOF MS of $d(CGG)_{10}$ was measured in the absence and presence of **NC** (Figure 2). In the absence of **NC**, two ions corresponding to 5– ion of $d(CGG)_{10}$ ($[\mathbf{CGG}]^{5-}$) (m/z, found 1903.94; calcd. 1880.90) and 6– ion of $d(CGG)_{10}$ ($[\mathbf{CGG}]^{6-}$) (found 1572.13; calcd. 1567.25) (Figure 2a), respectively, were observed. Upon addition of six equivalents of **NC** to the duplex solution, two new ions corresponding to the 6– ion of 6:1 complex of **NC** and the $d(CGG)_{10}$ ($[\mathbf{CGG} + 6\mathbf{NC}]^{6-}$) (found 2073.37; calcd. 2070.48) and the 7– ion of 6:1 complex of **NC** and the $d(CGG)_{10}$ ($[\mathbf{CGG} + 6\mathbf{NC}]^{7-}$) (found 1776.92; calcd. 1774.55) appeared. This result clearly showed that **NC** could bind to CGG trinucleotide repeat.

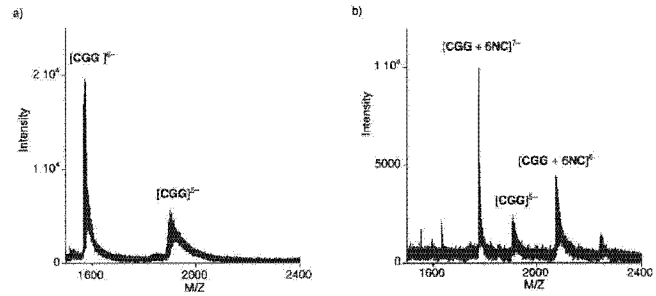

Figure 2. CSI-TOF mass spectra of $d(CGG)_{10}$ in the absence and presence of **NC**. Samples contained 20 μM duplex in 50% aqueous methanol and 100 mM ammonium acetate. For clarity, the range of m/z from 1500 to 2400 was shown. The sample solution was cooled at –10 °C during the injection with a flow rate of 0.5 mL/h. Key: (a) duplex only and (b) duplex with 120 μM **NC**.

CONCLUSION

All of the above data showed that the ligand **NC** could selectivity bind to the G-G mismatch. **NC** bound to CGG/CGG triad with an exclusive stoichiometry of 2:1 fashion. **NC** bound to CGG trinucleotide repeat could be thought as molecular label.

REFERENCES

1. Wells, R. D. and Warren, S. T. *Genetic Instabilities and Hereditary Neurological Diseases*; Academic Press: New York, 1998.
2. Gacy, A. M., Goellner, G., Juranic, N., Macura, S. and McMurray, C. T. *Cell* **1995**, *81*, 533-540.
3. Nakatani, K.; Sando, S. and Saito, I. *Nat. Biotechnol.* **2001**, *19*, 51-55.
4. Nakatani, K.; Sando, S.; Kumasawa, H.; Kikuchi, J. and Saito, I. *J. Am. Chem. Soc.* **2001**, *123*, 12650-12657.
5. Ghosh, A. K.; Duong, T. T.; McKee, S. P. and Thompson, W. J. *Tetrahedron Lett.* **1992**, *33*, 2781-2784.

Nucleic Acids Symposium Series No. 49 261–262

Application of L-DNA as a molecular tag

Gosuke Hayashi[1], Masaki Hagihara[2] and Kazuhiko Nakatani[2]

[1]Graduate School of Engineering, Kyoto University, Kyoto, 615-8246, Japan and [2]The Institute of Scientific and Industrial Research, Osaka University, Ibaraki, 567-0047, Japan

ABSTRACT

Enantiomeric DNA termed as L-DNA has unique properties. One is the ability of hybridizing to the complementary DNA as natural D-DNA. Another property is that the L-DNA could be recognized much more weakly by enzymes than D-DNA. We have focused our attention on these properties and applied L-DNA as a molecular tag. Here, we report that L-D chimera DNA is useful for PCR primers and subsequent separation and hybridization. Precise investigation revealed that in the process of PCR, L-DNA region could not be the PCR template and the polymerase extension reaction stopped at the boundary between L- and D-DNA region. As a result, L-DNA region formed like a "sticky end" and played a role of molecular tag. According to the L-DNA tag sequence, the produced L-DNA-tagged PCR products were easily separated or hybridized on the solid surface where the complementary L-DNA was pre-immobilized.

INTRODUCTION

L-DNA is an enantiomer of natural form of D-DNA. In biological systems, L-DNA and D-DNA mostly behave differently because, when L-DNA bound to proteins, sugars and nucleic acids, the produced complexes were diastereomeric to those produced from D-DNA. We have focused on the chemical properties of L-DNA and studied the application of L-DNA as a molecular tag in DNA microarray technology. DNA microarray is important tools for the biological studies. One drawback in current microarray technology is the lack of methods to directly immobilize the duplex DNA, e.g. PCR products on the array surface. We here show a chimera DNA consisting of L- and D-DNA are useful primers for PCR reaction and subsequent immobilization of duplexes on the array surface.

RESULTS AND DISCUSSION

The L-deoxynucleoside phosphoramidite units L-dT, L-dC, L-dA and L-dG were prepared according to the literatures[3, 4] (Scheme 1). The L-deoxyribose derivative **2** was synthesized from L-arabinose **1** through 8 steps. The L-deoxynucleosides were obtained by a glycosylation of appropriate nucleobase derivatives with compound **2**. After derivatization to nucleoside phosphoramidites, they were incorporated into L-D chimera oligodeoxynucleosides,

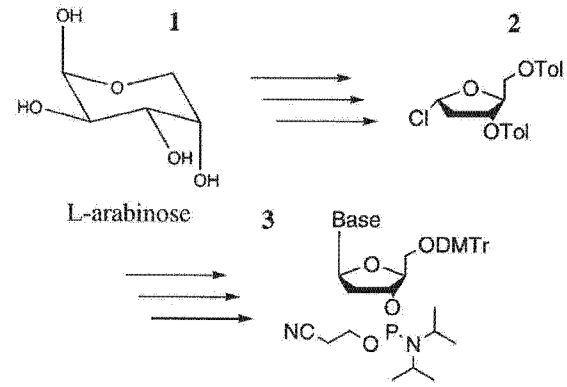

Scheme 1. Outline of synthesis scheme of L-deoxynucleoside phosphoramidite unit

d^{L}(GACAACGGAGACAGAGCAATTT)^{D}(CAATACGGGATAATACC) by a solid phase DNA synthesis method. This L-D chimera oligomer was purified by reverse phase HPLC and polyacrylamide gel electrophoresis (PAGE), and identified by MALDI-TOFMS. This oligomer consists of functionally two separated regions, D- and L-DNA; D-DNA region is served as primer for PCR and L-DNA region is served as a molecular tag. In the digestion experiment with the mixture of P1 nuclease and alkaline phosphatase, L-DNA region was little digested, although

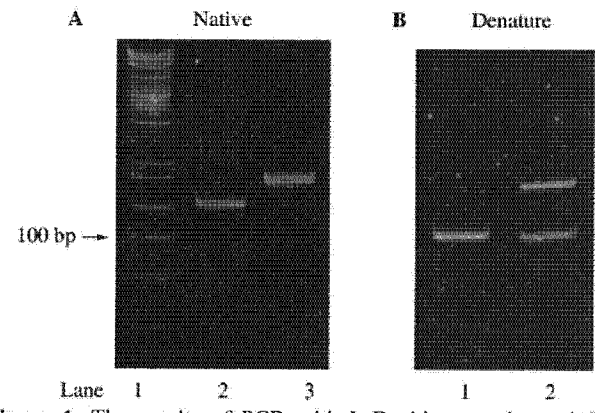

Figure 1. The results of PCR with L-D chimera primer. (**A**) 10 % native PAGE analysis of the PCR product; lane 1, DNA marker, lane 2, PCR product from normal primer consisting of only D-DNA, lane 3, PCR product from L-D chimera primer. (**B**) 8 % denaturing urea PAGE analysis of the PCR product; lane 1, PCR product from normal primer consisting of only D-DNA, lane 2, PCR product from L-D chimera primer

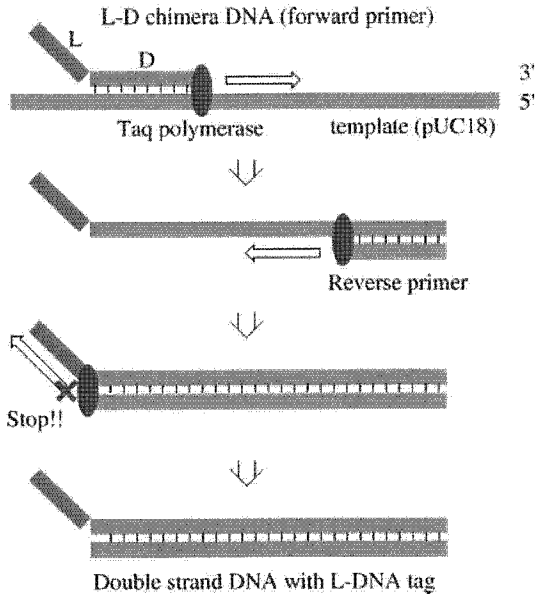

Figure 2. Schematic depiction of the polymerase extension reaction. Extension reaction starting from reverse primer stops at the boundary between L- and D-DNA region.

D-DNA region was completely digested to nucleotides. This result is consistent with L-DNA property.

With L-D chimera DNA in hand, the amplification reaction was carried out with 500 nM primers, Taq polymerase Master Mix (QIAGEN), 100 pg/μl template (puC18), for 35 cycles of 94°C x 30 sec, 55°C x 30 sec, 72°C x 1 min. The reaction mixture was analyzed by PAGE (Figure 1). A major product was observed in 140-150 bp region in lane 3, and its length is longer than normal PCR product, which was generated with normal forward primer from D-deoxyoligonucleotides, d^D(CAATACGGGATAATACC) (Figure 1A). In denaturing urea PAGE, two bands were clearly observed and the shorter band was the same length with normal PCR product (Figure 1B). This result suggested that in the process of PCR, L-DNA region could not be the PCR template and the polymerase extension reaction stopped at the boundary between L- and D-DNA region to obtain PCR product labelled by L-DNA (Figure 2). Further investigation using MALDI-TOFMS ensured that Taq polymerase could not elong even one nucleosides on L-DNA template.

The produced L-DNA tagged PCR products were exposed to SPR gold surface where L-DNA complementary with L-DNA tag were pre-immobilized. Two L-DNA having different sequence complementary with L-DNA tag part were immobilized on SPR gold chip through conventional method[6]. The address specific increase of SPR signal means that according to sequence information of L-DNA tagged PCR products, they hybridized to complementary L-DNA immobilized on SPR sensor chip. Thus, double strand DNA could be hybridized directly on the solid surface immobilizing L-DNA.

CONCLUSIONS

In these studies, usage of L-D chimera DNA as PCR primers leads to the formation of L-DNA tagged PCR products, which are very useful for immediate immobilization to the micro array. This novel method enables us to separate the multiple PCR products without any difficulties. This study is the first example for application of L-DNA to gene engineering.

ACKNOWLEDGEMENTS

We are grateful to the biotechnology group of TOYOBO Tsuruga Institute for excellent supports and advices.

REFERENCES

1. Williams, K. P., Liu, X., Schumacher, T. M., Lin, H., Ausiello, D. A., Kim, P. S. and Bartel, D. P. (1997) *Proc. Natl. Acad. Sci. USA*, **94**, 11285-11290.
2. Purschke, W. G., Radtke, F., Kleinjung, F. and Klussmann, S. (2003) *Nucleic Acid Res.*, **31**, 3027-3032.
3. Urata, H., Ogura, E., Shinohara, K., Ueda, Y. and Akagi, M. (1992) *Nucleic Acid Res.*, **20**, 3325-3332.
4. Shi, ZD., Yang, BH. and Wu YL. (2002) *Tetrahedron*, **50**, 3287-3296.
5. Hirschhorn, J. N., Skalr, P., Lindblad-Toh, K., Lim, Y., Ruiz-Gutierrez, M., Bolk, S., Langhorst, B., Schaffner, S., Winchester, E. and Landerm E. S. (2000) *Proc. Natl. Acad. Sci. USA*, **97**, 12164-12169
6. Kyo, M., Yamamoto, T., Motohashi, H., Kamiya, T., Kuroita, T., Tanaka, T., Engel, J. D., Kawakami, B. and Yamamoto, M. (2004) *Genes to Cells*, **9**, 153-164

Available online at www.sciencedirect.com
SCIENCE DIRECT
Bioorganic & Medicinal Chemistry
ELSEVIER
Bioorganic & Medicinal Chemistry 14 (2006) 5384–5388

Evaluation of mismatch-binding ligands as inhibitors for Rev–RRE interaction

Kazuhiko Nakatani,[a,b,*] Souta Horie,[a] Yuki Goto,[a] Akio Kobori[a,†] and Shinya Hagihara[a,‡]

[a]*Department of Synthetic Chemistry and Biological Chemistry, Faculty of Engineering, Kyoto University, Kyoto 615-8510, Japan*
[b]*The Institute of Scientific and Industrial Research (SANKEN), Osaka University, 8-1 Mihogaoka, Ibaraki 567-0047, Japan*

Received 18 January 2006; revised 20 March 2006; accepted 21 March 2006
Available online 5 April 2006

Abstract—Drugs targeting the stem-loop IIB of Rev responsible element (RRE) of HIV-1 mRNA are potential therapeutic agents for HIV-1 infection. The stem loop is characterized by an internal loop consist of consecutive G-G and G-A mismatches, which is the single binding site for Rev protein for nuclear export of viral mRNA. We report here that ligands binding to G-G and G-A mismatches in duplex DNA also bind to the internal loop in competition with Rev peptide and lead to the dissociation of pre-formed Rev–RRE complex in a model system.

1. Introduction

The Rev responsible element (RRE) of HIV-1 mRNA is a large RNA structure residing within the region that codes envelope proteins[1] and serves as a docking site for the Rev protein.[2,3] Binding of the Rev protein to RRE induces the nuclear export to the cytoplasm of unspliced or partially spliced viral mRNA. Interference in the formation of the Rev–RRE complex inhibits nuclear transport of the unspliced mRNA, eventually causing suppression of HIV-1 replication. An internal loop in stem-loop IIB of RRE has been identified as a single high-affinity site for the Rev binding[4,5] (Chart 1). Thus, small molecular ligands that bind to the loop in competition with Rev protein are potential therapeutic agents for treating HIV-1 infection.[6–8]

However, the design of RNA targeting molecules still remained to be a challenge in medicinal chemistry because of the complicated RNA secondary and tertiary structures.[9–11] We have discovered a novel class of compounds that bind selectively to the mismatched base pair in duplex DNA. The stem-loop IIB of HIV-1 RRE is characterized by an internal loop consisting of two consecutive mismatched base pairs, one a G-G mismatch and the other a G-A mismatch. These non-Watson–Crick base pairs have been shown to be responsible for the Rev binding. We here report that naphthyridine dimer (**ND**)[12,13] and naphthyridine–azaquinolone (**NA**)[14,15] which bind to the G-G and G-A mismatches in duplex DNA, respectively, are the potential candidates of drug lead that inhibits the Rev–RRE interaction (Chart 2).

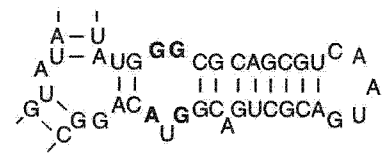

stem-loop IIB of HIV-1 RRE

Chart 1. A structure of stem-loop IIB of HIV-1 mRNA.

2. Results and discussion

We first qualitatively evaluated the binding of **ND** and **NA** to various RNA structures using surface plasmon resonance (SPR) assay with the sensors carrying **ND**

Keywords: RNA recognition; Inhibitors; Drug design; HIV-1 RRE.
* Corresponding author. Tel.: +81 6 6879 8455; fax: +81 6 6879 8459; e-mail: nakatani@sanken.osaka-u.ac.jp
† Present address: Department of Polymer Science and Engineering, Kyoto Institute of Technology, Matsugasaki, Sakyo-ku, Kyoto 606-8585, Japan.
‡ Present address: RIKEN (The Institute of Physical and Chemical Research), 2-1 Hirosawa, Wako-shi, Saitama 351-0198, Japan.

0968-0896/$ - see front matter © 2006 Elsevier Ltd. All rights reserved.
doi:10.1016/j.bmc.2006.03.038

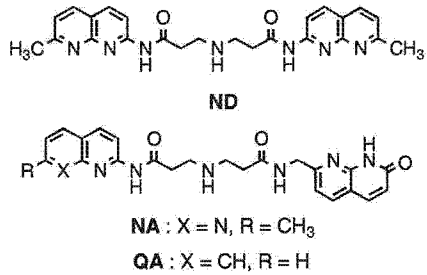

Chart 2. Structures of ligands used in these studies.

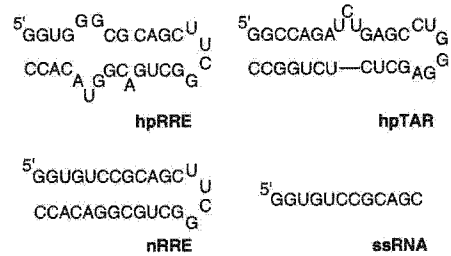

Chart 4. RNAs used in these studies and their possible secondary structures.

and **NA** on the surfaces. **ND** was immobilized as **aminolink-ND** at the secondary nitrogen by way of a short aminoalkyl linker onto the surface of carboxymethyl dextran of a CM5 sensor chip (BIAcore) (Chart 3).[12] **NA** was immobilized as a form of amino-linked dimer (**aminolink-NA**) to increase a surface density of the ligand,[15] because the **NA**-binding to a G-A mismatch in RNA was anticipated to be weaker than the **ND**-binding to a G-G mismatch based on their bindings to the mismatches in duplex DNA. Using the **ND**-immobilized sensor, a strong SPR response was observed for a hairpin RNA (**hpRRE**) (Chart 4) representing the stem-loop IIB of HIV-1 RRE (Fig. 1a). In contrast, a completely matched hairpin RNA (**nRRE**), which lacked an internal loop consisting of the G-G and G-A mismatches, did not bind to the **ND**-immobilized sensor surface. Very weak binding was observed for a single stranded RNA (**ssRNA**) and a hairpin RNA representing TAR RNA of HIV-1 (**hpTAR**) containing the r(UCU) bulge. SPR analyses with **NA**-immobilized surfaces showed a strong SPR response for **hpRRE**, whereas virtually no responses for other three RNAs (Fig. 1b). These experiments demonstrated that both **ND** and **NA** did not bind to a completely matched RNA duplex, r(UUCG) and r(CUGGGA) hairpin loops, and a r(UCU) bulge. Thus, the internal loop consisting of the G-G and G-A mismatches in **hpRRE** is most likely the binding site of both **ND** and **NA**.

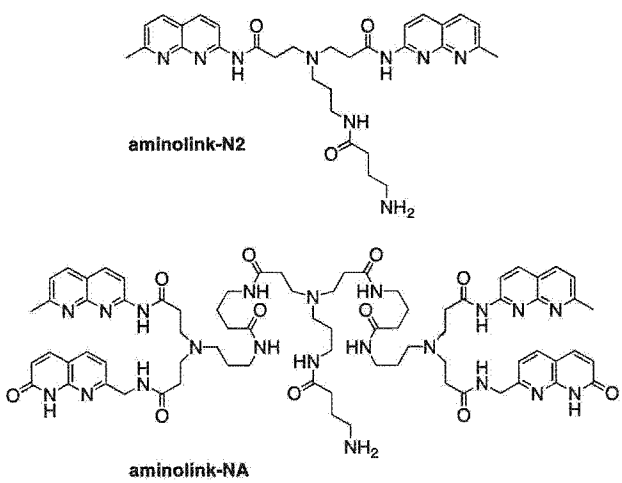

Chart 3. Structures of **aminolink-ND** and **aminolink-NA** used for the immobilization of **ND** and **NA**, respectively, onto the SPR sensor surface.

Separate experiments showed that **ND**-binding to the G-G mismatches in duplex RNA was favorable for those flanked by a single nucleotide bulge. (Table 1) The increase of T_m (ΔT_m) of G-G mismatch RNA duplex was 4.8 °C, whereas it increased up to 9.1 °C when the G-G mismatch was flanked by a single uridine and adenine bulge. Since the single uridine and adenine bulge in RNA duplex was not the site of the **ND** binding, it is most likely that structural perturbation on the G-G mismatch by the neighboring nucleotide bulge favorably affected the **ND**-binding to the G-G mismatch in RNA duplexes. The RNA duplex is known to have A-form, which has a deep major groove compared to that of B-form DNA duplex. **ND** binds to the G-G mismatch from the major groove side of DNA duplex. Thus, the single nucleotide bulge flanking the G-G mismatch may loosen the deep major groove to facilitate the **ND**-binding.

The binding of **ND** and **NA** to the stem-loop IIB of RRE was examined with respect to the structure of the heterocycles in the ligand. We measured the difference in the absorption spectra of ligands between the absence and presence of **hpRRE**. The absorption of unbound **ND** at 320 nm decreased with a concomitant bathochromic shift as indicated by an increased absorption at 345 nm (Fig. 2a). Similar changes in the UV spectra were observed for **NA** with a decreased efficiency. Bathochromic shifts of the ligand absorptions suggested the stacking interaction of bound **ND** and **NA** with the neighboring bases in **hpRRE**. In contrast, a ligand, aminoquinoline–azaquinolone (**QA**), which did not bind to the G-G and G-A mismatches in duplex DNA,[14] showed little absorption change in the spectra. A complete loss of binding as observed for **QA** suggested an important role of 2-aminonaphthyridine for the binding to **hpRRE**. The UV absorption change of these ligands in the presence of **nRRE** was quite small with virtually no bathochromic shift, strongly suggesting that the internal loop in **hpRRE** would be the site of binding of **ND** and **NA** (Fig. 2b).

Having the data indicating the binding of **ND** and **NA** to **hpRRE**, we investigated competitive binding of these molecules with the Rev model peptide 5,6TAMRA-TRQARRNRRRRWRERQRAAAAK-amide (**tamRev**) by fluorescence anisotropy displacement assay.[6,16] The peptide consisted of an arginine-rich motif (Rev_{34-50}) and an alanine-rich sequence, and was previously shown to interact with high affinity to RRE stem-loop IIB.[6,17]

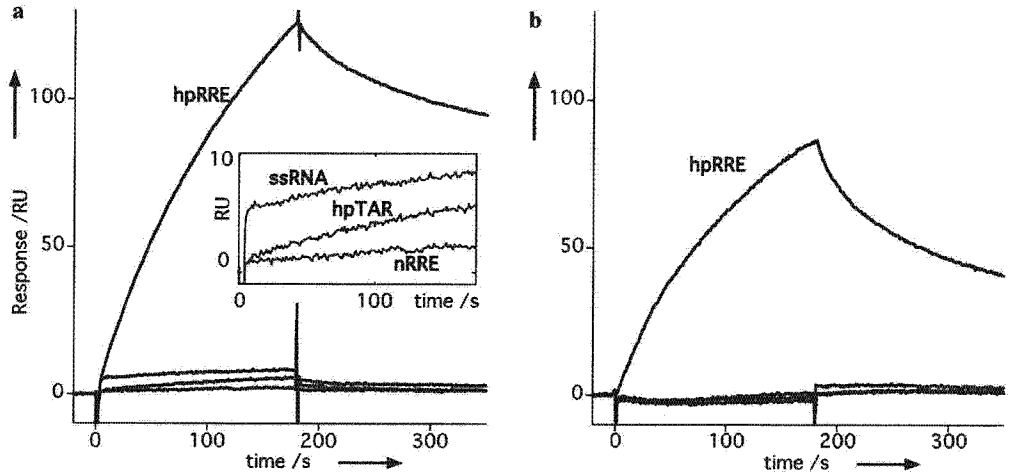

Figure 1. SPR assays of RNA-binding to the ligand-immobilized sensor surfaces. RNA sample (**hpRRE**, **nRRE**, **hpTAR**, and **ssRNA**, each 100 nM) in 10 mM HEPES and 150 mM NaCl was heat denatured, folded by slow cooling, and applied to the sensor for 180 s with a flow rate of 30 μL/min. (a) **ND**-immobilized sensor surface. Inset: expansion of the responses from 0 to 10 RU. The amount of **ND** immobilized on the surface was 370 RU. (b) **NA**-immobilized sensor surface. The amount of **NA** immobilized on the surface was 1900 RU.

Table 1. Melting temperature (T_m) of RNA in the absence of **ND**

RNA sequence	T_m (°C)		ΔT_m (°C)
	RNA	RNA + **ND**	
5′-r(CUAACGGAAUG)-3′ 3′-r(GAUUGCCUUAC)-5′	48.7	47.9	−0.8
5′-r(CUAACGGAAUG)-3′ 3′-r(GAUUGGCUUAC)-5′	33.5	38.3	4.8
5′-r(CUAACG GAAUG)-3′ 3′-r(GAUUGC CUUAC)-5′ **U**	36.0	36.5	0.5
5′-r(CUAACG GAAUG)-3′ 3′-r(GAUUGC CUUAC)-5′ **A**	35.1	35.2	0.1
5′-r(CUAACG GAAUG)-3′ 3′-r(GAUUGG CUUAC)-5′ **U**	30.6	39.7	9.1
5′-r(CUAAC GGAAUG)-3′ 3′-r(GAUUG GCUUAC)-5′ **U**	29.3	38.1	8.8
5′-r(CUAACG GAAUG)-3′ 3′-r(GAUUGG CUUAC)-5′ **A**	26.4	35.0	8.6
5′-r(CUAAC GGAAUG)-3′ 3′-r(GAUUG GCUUAC)-5′ **A**	26.8	35.4	8.6

The UV–melting curves were measured for duplexes (4 μM) in 10 mM sodium cacodylate buffer (pH 7.0) containing 100 mM NaCl in the absence and presence of ND (100 μM). Temperature was increased at a rate of 1 °C/min.

The N-terminal was fluorescently labeled with 5,6-TAMRA, whereas C-terminal was amidated. Upon addition of **hpRRE**, fluorescence anisotropy of **tamRev** (100 nM) increased markedly with increasing concentrations of **hpRRE** up to 160 nM, above which anisotropy exhibited a plateau, indicating formation of a complex (**tamRev–hpRRE**) (Fig. 3a). Using a nonlinear regression analysis of the binding curve reported earlier,[6,18] the dissociation constant of the **tamRev–hpRRE** complex was determined to be 5.6 nM. To examine inhibitory activities of the ligands on the formation of the **tamRev–hpRRE** complex, we measured the decrease in fluorescence anisotropy of a pre-formed **tamRev–hpRRE** complex upon titrating with the ligands. A release of bound **tamRev** from the complex by ligand displacement resulted in a decrease of fluorescence anisotropy. Upon titrating the **tamRev–hpRRE** complex with **ND**, **NA**, and neomycin B, a decrease in fluorescence anisotropy was

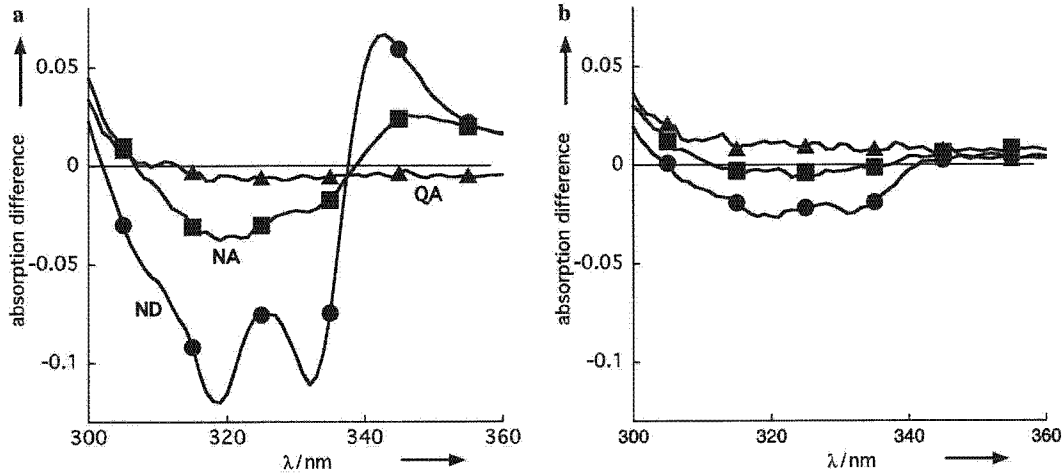

Figure 2. Difference UV spectra of ligands (20 μM) in the presence of (a) **hpRRE** (2 μM) and (b) **nRRE** (2 μM) in sodium phosphate (pH 7.0) containing EDTA (1 mM) and NaCl (100 mM). Key: **ND** (circle); **NA** (square); **QA** (triangle).

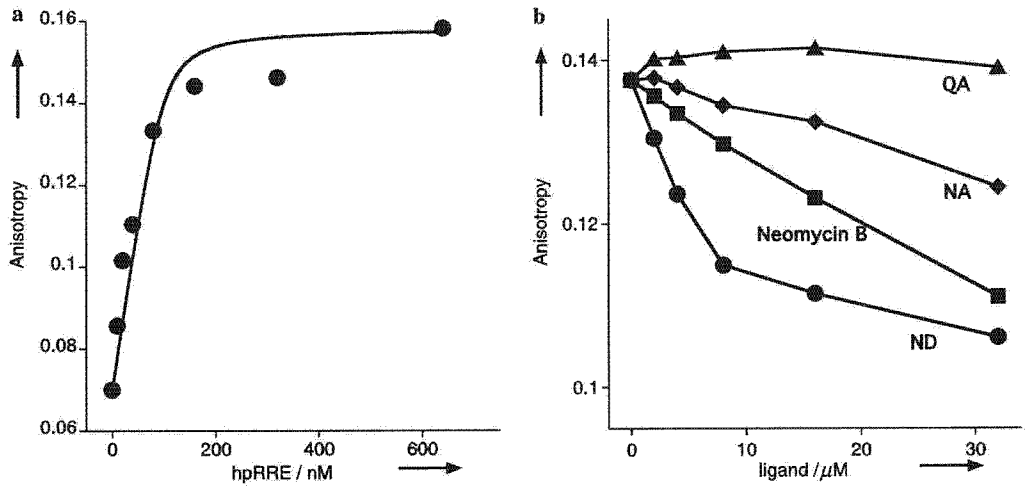

Figure 3. Fluorescence anisotropy assay. (a) A change of fluorescence anisotropy of **tamRev** (100 nM) (circle) titrated with **hpRRE**. Concentrations of **hpRRE** were 0, 10, 20, 40, 80, 160, 320, and 640 nM. The solid line represents a calculated binding curve obtained by a nonlinear regression analysis of the raw data. (b) Decreases of anisotropy by titrating the pre-formed complex between **hpRRE** (100 nM) and **tamRev** (100 nM) with ligands. Ligand concentrations were 0, 2, 4, 8, 16, and 32 μM. Key: **ND** (circle), **NA** (diamond), neomycin B (square), and **QA** (triangle).

observed, but not with **QA** (Fig. 3b). The dissociation of the **tamRev–hpRRE** complex was induced by **ND** much more efficiently than by neomycin B and **NA**.

3. Conclusion

The data reported here showed that (1) ligands binding to G-G and G-A mismatches in duplex DNA could also bind to a stem-loop IIB of RRE and (2) **ND** showed a stronger inhibitory activity for **tamRev–hpRRE** formation than neomycin B. While the precise mode of the binding as well as the binding stoichiometry of **ND** could not be determined by SPR and mass spectrometry, **ND** and **NA** were found useful to capture HIV-1 RRE when these molecules were immobilized on the surface. In addition, these results suggested that structural optimization of **ND** and **NA** toward the binding to the internal loop may lead molecules showing potent inhibitory activities against Rev–RRE binding.

4. Experimental

4.1. Substrates

All RNAs were purchased from PROLIGO with HPLC purification. 5,6-TAMRA-labeled peptide model was custom synthesized by Biosource International Inc. (Camarillo, California) with a purity of >95%.

4.2. General procedure for SPR-binding experiments

All measurements were carried out at 25 °C in a continuous flow of HBS-N buffer (10 mM HEPES, pH 7.4) containing NaCl (150 mM) at a flow rate of

30 μL/min. RNA samples (0.1 μM) in HBS-N buffer were heat denatured, folded by slow cooling, and injected into the sensor for 3 min to analyze the association to the surface. Then, the dissociation of the bound RNA to the surface was analyzed by injecting buffer only.

4.3. UV measurements

All UV measurements were carried out with SHIMADZU UV-2550 (Kyoto, Japan) at 25 °C.

4.3.1. Sample preparation. hpRRE, hpTar, ssRNA, and nRRE (2 μM) were denatured at 90 °C and cooled down slowly to a room temperature in a buffer (3.75 mM Na-phosphate, pH 7.0, 100 mM NaCl, 1.0 mM EDTA). A solution of ligand (20 μM) was added to the solution and left for 1 h at 25 °C. UV spectra were measured for each ligand with or without RNA. The difference UV spectra were obtained by subtracting the data in the presence of RNA from the data in the absence of RNA.

4.4. Fluorescence anisotropy assay

Fluorescence Anisotropy assays were carried out with a Beacon2000 system (Invitrogen) at 25 °C.

4.4.1. tamRev–hpRRE binding. hpRRE was denatured at 90 °C and cooled down slowly to a room temperature in a buffer (30 mM HEPES, pH 7.5, 10 mM Na-phosphate, pH 7.5, 100 mM KCl, 10 mM NH_4OAc, 0.1% Nonidet NP-40, 10 mM guanidine·HCl, 2 mM $MgCl_2$, 20 mM NaCl, 0.5 mM EDTA). To the solution of variable concentrations of **hpRRE** (10, 20, 40, 80, 160, 320, and 640 nM), **tamRev** (100 nM) was added and left for 12 h at 25 °C. Fluorescence anisotropy of the complex was measured with Beacon2000 at 25 °C. Average read cycles for the measurements were set to 10. The range control was auto.

4.4.2. Inhibition assay. tamRev–hpRRE complex was prepared by mixing 100 nM of each **tamRev** and **hpRRE** in a buffer as described above. A varing concentration of ligand (2, 4, 8, 16, and 32 μM) was added to the solution of **tamRev–hpRRE**, and the whole solution was left at 25 °C for 12 h. Fluorescence anisotropy was measured as above.

4.4.3. Curve fitting. Non-linear regression analysis for the **tamRev–hpRRE** formation was carried out by SigmaPlot2001 by using the equation for the 1:1 binding as shown below:

$$A_{obs} = (A_{max} - A_0) \cdot \alpha + A_0,$$

$$\alpha = \frac{([Rev]_0 + [RRE]_0 + K_d) \pm \sqrt{([Rev]_0 + [RRE]_0 + K_d)^2 - 4 \cdot [Rev]_0 \cdot [RRE]_0}}{2 \cdot [Rev]_0},$$

where A_0 and A_{max} are anisotropy observed at 0 and 600 nM of **hpRRE**. $[Rev]_0$ and $[RRE]_0$ are the total concentration of each. K_d is the dissociation constant, whereas α is the molar fraction of Rev–RRE complex against $[Rev]_0$.

Acknowledgment

Authors thank Dr. Fumie Takei for the experimental assistance.

References and notes

1. Pollard, V. M.; Malim, M. H. *Annu. Rev. Microbiol.* **1998**, *52*, 491–532.
2. Malim, M. H.; Böhnlein, S.; Hauber, J.; Cullen, B. R. *Cell* **1989**, *58*, 205–214.
3. Daly, T. J.; Cook, K. S.; Gray, G. S.; Maione, T. E.; Rusche, J. R. *Nature* **1989**, *342*, 816–819.
4. Bartel, D. P.; Zapp, M. L.; Green, M. R.; Szostak, J. W. *Cell* **1991**, *67*, 529–536.
5. Iwai, S.; Pritchard, C.; Mann, D. A.; Karn, J.; Gait, M. J. *Nucleic Acids Res.* **1992**, *20*, 6465–6472.
6. Luedtke, N. W.; Tor, Y. *Angew. Chem., Int. Ed.* **2000**, *39*, 1788–1790.
7. Kirk, S. R.; Luedtke, N. W.; Tor, Y. *J. Am. Chem. Soc.* **2000**, *122*, 980–981.
8. Hendrix, M.; Priestley, E. S.; Joyce, G. F.; Wong, C.-H. *J. Am. Chem. Soc.* **1997**, *119*, 3641–3648.
9. Zaman, G. J. L.; Michiels, P. J. A.; van Boeckel, C. A. A. *Drug Discovery Today* **2003**, *8*, 297–306.
10. Gallego, J.; Varani, G. *Acc. Chem. Res.* **2001**, *34*, 836–843.
11. Tok, J. B. H.; Bi, L. R.; Saenz, M. *Bioorg. Med. Chem. Lett.* **2005**, *15*, 827–831.
12. Nakatani, K.; Sando, S.; Saito, I. *Nat. Biotechnol.* **2001**, *19*, 51–55.
13. Nakatani, K.; Sando, S.; Kumasawa, H.; Kikuchi, J.; Saito, I. *J. Am. Chem. Soc.* **2001**, *123*, 12650–12657.
14. Hagihara, S.; Kumasawa, H.; Goto, Y.; Hayashi, G.; Kobori, A.; Saito, I.; Nakatani, K. *Nucleic Acids Res.* **2004**, *32*, 278–286.
15. Nakatani, K.; Hagihara, S.; Goto, Y.; Kobori, A.; Hagihara, M.; Hayashi, G.; Kyo, M.; Nomura, M.; Mishima, M.; Kojima, C. *Nat. Chem. Biol.* **2005**, *1*, 39–43.
16. Luedtke, N. W.; Tor, Y. *Biopolymers* **2003**, *70*, 103–119.
17. Lacourciere, K. A.; Stivers, J. T.; Marino, J. P. *Biochemistry* **2000**, *39*, 5630–5641, With a short RRE construct, neomycin showed K_i value of 2 μM for inhibition of Rev binding. The highest affinity site of RRE for neomycin-binding (K_d = 0.24 μM) was not disruptive to Rev-binding.
18. Sevenich, F. W.; Langowski, J.; Weiss, V.; Rippe, K. *Nucleic Acids Res.* **1998**, *26*, 1373–1381.

DNA Hybridization

DOI: 10.1002/anie.200601190

Mismatch-Binding Ligands Function as a Molecular Glue for DNA**

*Tao Peng, Chikara Dohno, and Kazuhiko Nakatani**

Single-stranded DNA (ssDNA) hybridizes with another ssDNA unit having the complementary base sequence. The high sequence specificity in the hybridization is one of the most important properties of DNA as a genetic material, and also characterizes DNA as the unique component of the molecular architecture.[1–5] The formation of a double-stranded DNA (dsDNA) molecule of fully matched base sequences is highly energetically favorable and proceeds spontaneously at a temperature below the melting temperature (T_m) of the duplex, and therefore it is difficult to turn the hybridization on and off under isothermal conditions. Studies toward controlling or modulating the DNA hybridization with photochemical[6–9] and electronic reactions[10,11] of chemically modified oligonucleotides have been reported. Herein, we describe an approach to turn on duplex formation of two natural, unmodified ssDNA sequences that do not spontaneously hybridize with each other by a mismatch-binding ligand (MBL).

Recent studies on the binding of an MBL to the $(CGG)_n$ trinucleotide repeat revealed a novel mode of ligand binding to a mismatched DNA duplex.[12,13] The naphthyridine carbamate dimer (**NC**) selectively binds to the 5′-CGG-3′/5′-CGG-3′ sequence (CGG/CGG), which involves a G–G mismatch flanked by two C–G base pairs, with a 2:1 **NC**/DNA stoichiometry. The binding of **NC** to the CGG/CGG sequence induced two cytosines to be out of the π stack, as evidenced by the selective cleavage at the unpaired cytosine triggered by the addition of hydroxylamine.[12] We anticipated that the flipped-out cytosine in the **NC**-bound CGG/CGG triad could be substituted with other nucleotide bases such as thymine, and therefore **NC** could stabilize the 5′-TGG-3′/5′-TGG-3′ (TGG/TGG) sequence that consists of three contiguous T–G, G–G, and G–T mismatches (Figure 1). As the hybridization of two ssDNA molecules to produce the TGG/TGG sequence would be energetically unfavorable, these ssDNA sequences could be adhered by binding of **NC** to the TGG/TGG sequence.

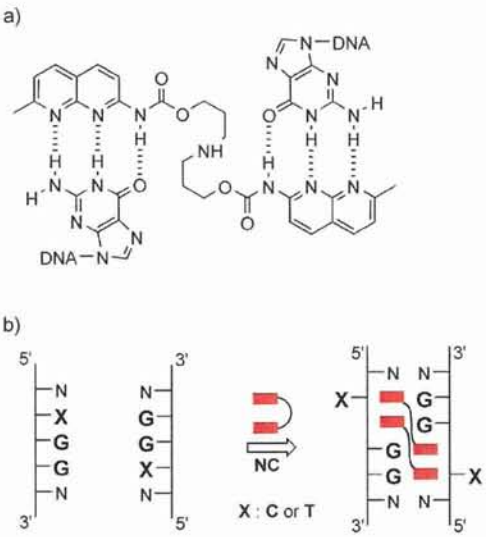

Figure 1. a) **NC** and its hydrogen-bonding pattern to a guanine–guanine mismatch. b) Schematic representation of the binding of **NC** to the XGG/XGG sequence. Red rectangles: naphthyridine rings.

The binding of **NC** was first investigated for 5′-TGG-3′/5′-CGG-3′ (TGG/CGG) where one cytosine of the CGG/CGG sequence was substituted with thymine. The 11-mers 5′-d(CCCATGGTCCG)-3′ (**T1**) and 5′-d(CGGACGGTGGG)-3′ (**C1**; 5 μM) produced a duplex (**T1/C1**) containing a TGG/CGG sequence with a T_m of 35.7 °C in sodium cacodylate buffer. In the presence of **NC**, the T_m of the **NC**-bound **T1/C1** was 71.1 °C, which shows an increase in T_m of 35.4 K (Figure 2). The transition from dsDNA to ssDNA is monophasic, regardless of the presence of **NC**. The transition occurred somewhat less cooperatively in the presence of **NC**. The melting kinetics may not be as simple as those in the

[*] Dr. T. Peng, Dr. C. Dohno, Prof. K. Nakatani
Department of Regulatory Bioorganic Chemistry
The Institute of Scientific and Industrial Research (SANKEN)
Osaka University
8-1 Mihogaoka, Ibaraki 567-0047 (Japan)
Fax: (+81) 6-6879-8459
E-mail: nakatani@sanken.osaka-u.ac.jp

[**] This work was supported by a Grant-in-Aid for Scientific Research (A) from the Japan Society for the Promotion of Science, Health and Labor Sciences Research Grants for Research on Advanced Medical Technology from the Ministry of Health, Labor, and Welfare, and CREST, Japan Science and Technology Agency.

Supporting information for this article is available on the WWW under http://www.angewandte.org or from the author.

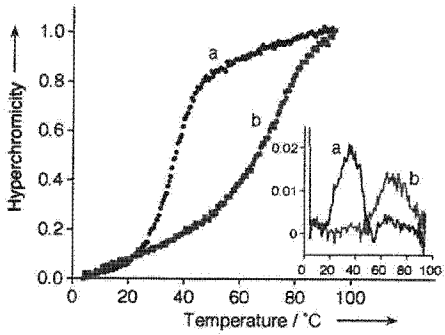

Figure 2. Thermal denaturation profile of **T1** and **C1** (5 μM each) in the absence (a) and presence (b) of **NC** (100 μM). The absorbance at 260 nm was measured in sodium cacodylate buffer (10 mM, pH 7.0) containing 0.1 M NaCl. The temperature was increased from 4 to 94 °C at a rate of 1 °C min^{-1}. The absorbance was measured with an interval of 1 °C. Measurements were carried out at least three times. The average of three data sets of denaturation profiles was used for the plots. Inset: differential plots of the melting profiles.

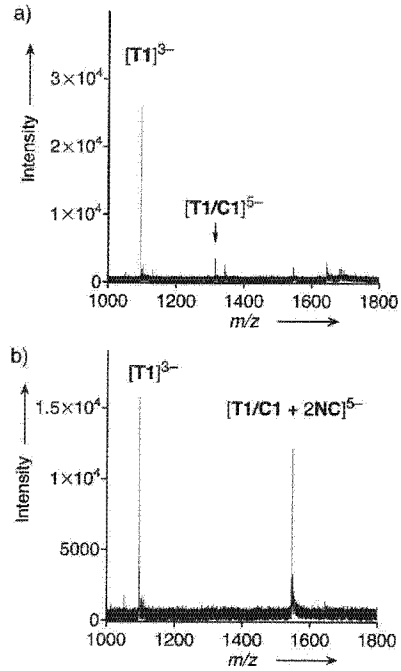

Figure 3. CSI-TOF MS of **T1** and **C1** in the a) absence and b) presence of **NC** (40 μM). Samples contained 20 μM of each strand in 50% aqueous methanol and ammonium acetate (100 mM). Ions in the range of *m/z* from 1000 to 1800 are shown for clarity. The sample solution was cooled at −10 °C during the injection with a flow rate of 0.5 mL h^{-1}.

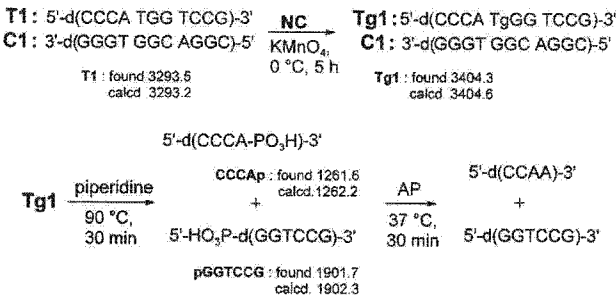

Scheme 1. The oxidation of **T1/C1** by $KMnO_4$ upon binding of **NC**. AP = alkaline phosphatase.

absence of **NC**, because this transition involves the dissociation of four components, two DNA strands (**T1** and **C1**) and two **NC** molecules. The thermal denaturation profiles showed that in the temperature range between 45 and 55 °C, **T1** and **C1** were present as single-stranded forms in the absence of **NC** but as an **NC**-bound duplex form in the presence of **NC**.

The cold-spray ionization time-of-flight mass spectrometry (CSI-TOF MS)[12,14] of **T1** and **C1** showed ions corresponding to a 3− ion of a single-stranded form ([**T1**]$^{3-}$, *m/z*: found: 1096.2; calcd: 1096.2) and a 5− ion of a duplex form ([**T1/C1**]$^{5-}$, *m/z*: found: 1344.8; calcd: 1344.6; Figure 3a). On addition of **NC** to the duplex with a 2:1 molar ratio, the intensity of the ions corresponding to [**T1**]$^{3-}$ became weaker with the concomitant appearance of a new ion corresponding to the 5− ion of a 2:1 complex of **NC** and the duplex ([**T1/C1** + 2**NC**]$^{5-}$, *m/z*: found: 1546.3; calcd: 1545.9; Figure 3b). On increasing the concentration of **NC**, the intensity of the ion corresponding to [**T1/C1** + 2**NC**]$^{5-}$ became strong with a concomitant decrease of the intensity of [**T1**]$^{3-}$ (see Supporting Information). Complexes of **NC** bound to **T1/C1** with 1:1 and/or 3:1 stoichiometries were not detected. These results clearly showed that the binding of **NC** to the duplex **T1/C1** proceeded in an exclusive stoichiometry of 2:1. This stoichiometry of **NC** binding is the characteristic feature that is observed for the binding of **NC** to the CGG/CGG sequence[12] and the binding of the related MBL naphthyridine azaquinolone to the CAG/CAG sequence. The structure of the latter complex has been determined by NMR spectroscopy.[13] These findings suggested that the thymine in the **NC**-bound **T1/C1** would most likely be out of the π stack.

The T component in the extrahelical position could be preferentially oxidized with potassium permanganate ($KMnO_4$) compared to that in the intrahelical position.[15] The resulting thymine glycol (Tg) can be degraded with hot piperidine, eventually leading to strand cleavage.[16–18] The oxidation of **T1/C1** with $KMnO_4$ followed by treatment with hot piperidine was examined (Scheme 1). The duplex **T1/C1** (12.5 μM) did not react with $KMnO_4$ (0.2 mM) at 0 °C for 320 min, as judged by reversed-phase HPLC analysis (see Supporting Information). In contrast, the TGG-containing DNA **T1** was consumed by 70% in the presence of **NC** (40 μM) and converted into the 11-mer DNA 5′-d(CCCA-TgGGTCCG)-3′ (**Tg1**) which contained a Tg unit.[16] After isolation by HPLC, **Tg1** was treated with hot piperidine to give two products corresponding to oligomers 5′-d(CCCA)-PO_3H-3′ (**CCCAp**) and 5′-HO_3P-d(GGTCCG)-3′ (**pGGTCCG**). All DNA products were identified by MALDI-TOF mass spectrometry (Scheme 1). Although the duplex **T1/C1** contained two kinds of thymine residues, only that in the TGG/CGG sequence was reactive to $KMnO_4$ upon **NC** binding. These results clarified the finding that the T unit in the TGG/CGG sequence was in the extrahelical position in the **NC**-bound complex.